Manuscript of final submission September 2018, printed in
"Energy" Vol. 165, Part B, 15 Dec 2018, pp. 1060-1071, doi.org/10.1016/j.energy.2018.10.034

Gas turbine exhaust gas heat recovery by organic Rankine cycles (ORC) for offshore combined heat and power applications - energy and exergy analysis

Hossein Nami[a,b]*, Ivar S. Ertesvåg[b], Roberto Agromayor[b], Luca Riboldi[b], Lars O. Nord[b]

[a]Faculty of Mechanical Engineering, University of Tabriz, 29th Bahman Blvd., 5166616471, Tabriz, Iran.

[b]Department of Energy and Process Engineering, NTNU Norwegian University of Science and Technology, Kolbjørn Hejes vei 1B, NO-7491, Trondheim, Norway.

*Corresponding author: h.nami@tabrizu.ac.ir

Abstract

Effective heat and power supply to offshore installations leads to environmental benefits, but the efficiency is often limited by requirements and constraints connected to the offshore environment. An exergetic analysis of gas turbines exhaust heat recovery on offshore platforms is performed to identify optimal approaches to produce heat and power. Two different configurations are presented, with heat delivery at two temperature levels and power production by an organic Rankine cycle (ORC). In one system (cascade), the high temperature heat is taken from the exhaust after the ORC, while low temperature heat is taken from the ORC condenser. Alternatively, high and low temperature heat is taken from the exhaust gas before the ORC feeds on the remaining exhaust thermal energy (series system). Four different working fluids (three siloxanes, one refrigerant) are considered. In addition, the exergetic effects of the heat loads and heat source temperatures are investigated. The results revealed that MM and R124 are the best working fluids for the cascade and series system, respectively. A recuperated ORC in the series

system improve the siloxane results, with MM as the best working fluid. Moreover, decreasing the ORC minimum pressure in the series system makes considerable improvement.

Keywords:

Oil & gas platforms

Waste heat recovery

Cogeneration

High-temperature ORC

Siloxane

1. Introduction

Oil and gas extraction from offshore petroleum fields is an energy intensive process, which consumes from 10 to several hundreds of megawatt of electrical power as well as heat [1]. The energy requirements are a function of the system design, the export specifications and the properties of the field. Normally, offshore facilities are designed for the maximum amount of oil and gas extraction [2]. When the hydrocarbon production decreases as the field ages, the power demand increases due to recovery techniques like water injection [3]. The common strategy to meet the varying power demand is to employ several local gas turbines with relatively low thermal efficiency. The thermal energy available in the exhaust gas is then harvested by waste heat recovery units to provide heat to the platform. This basic layout has obvious advantages in terms of high operational flexibility and ease of implementation. However, significant room for improvements was identified as other concepts showed potential to achieve better performance [4]. Efficiency improvements were identified as a sustainable option to simultaneously satisfy

economics and energy security as well as the environmental objectives [5]. Considering the thermodynamic performance of petroleum platforms, efficiency increase is achievable through improving the performance of the processing plant, e.g. by decreasing irreversibility in heat exchangers [6]–[8], as well as the efficiency of the utility plant, e.g. by bottoming cycles [9]–[12]. Although the second route has been the subject of different studies, it has limitations for offshore facilities. For example, integration of steam cycles (as a bottoming cycle) in offshore facilities is not common due to the high cost to weight ratio of the equipment. To make the concept viable, the additional investment costs associated with the supplementary weight and space have to be outweighed by the financial gain of exporting a higher amount of hydrocarbons and of emitting less CO_2. A compact combined cycle had a weight-to-power ratio 60-70% higher than that of a simple gas turbine [10]. On the other hand, organic Rankine cycles (ORCs) have some considerable advantages in comparison with steam cycles, such as operating at lower pressures, having lower operating/maintenance cost and being adaptable to low/medium grade heat sources [13]–[15]. In recent years, waste heat recovery from offshore fields via ORCs has been the focus of attention, although there is no practical case. The following literature review represents some of the most recent research in this subject.

Barrera et al. [16] investigated exergetic performance of a Brazilian floating oil platform equipped with ORC. They used cyclopentane as the working fluid and determined the best configuration of the ORC based on its vapor saturation curve. It was found that the output power, utilizing the exhaust gas exergy, was considerable, and that the ORC saved 15 – 20% of the fuel consumption. For the case of the Draugen offshore platform in the North Sea, a proposed waste heat recovery by an ORC from the Siemens SGT-500 gas turbine installed on the field was studied by Pierobon et al. [17]. Using a genetic algorithm, the performance of the ORC was

optimized considering some decision variables, i.e. the working fluid, the evaporator pressure and temperature, the pinch points and the temperatures and velocities in the heat exchangers. Their optimization resulted in choosing cyclopentane and acetone as the proposed optimal working fluids, where cyclopentane had a higher thermal efficiency compared with acetone. A cogeneration system producing power, heating and fresh water from waste heat at a Persian Gulf offshore field was outlined and analyzed by Eveloy et al. [18]. They recovered thermal energy of the exhaust gas using an ORC, which ran a reverse osmosis desalination system. In addition, condensation heat rejected from the ORC was used for process heating. They showed that the combination of the cogeneration system (with MDM as the ORC working fluid) led to a 6 MW net power output, 1380 m^3/hour of fresh water and 37 MW of process heat. This increased the gas turbine exergetic efficiency by 6%. In a case study, Khatita et al. [19] analyzed basic and recuperated ORCs in order to recover the waste heat and convert it into power in an existing gas treatment section in Egypt. They made use of several working fluids in their simulations to consider the effects on the system decision parameters like net output power and efficiency. According to this study, a recuperated cycle with either benzene or cyclohexane as working fluids can be the most promising option. A comprehensive assessment of bottoming ORC based waste heat recovery from a wide range of gas turbines, with power ratings generally employed offshore, was conducted by Bhargava et al. [20]. Two kinds of thermal connection between the gas turbine exhaust gas and the ORC were considered, namely with and without a secondary heat transfer fluid. They used cyclopentane and Dowtherm-A as the ORC working fluid and heat transfer fluid, respectively. These authors found that compared to direct evaporation, the intermediate (secondary) heat transfer fluid had some practical benefits, however, gave poorer thermodynamics performance.

The review of the relevant literature showed that many aspects related to the utilization of offshore combined cycles have been thoroughly investigated. However, two main gaps were identified in the body of knowledge. First, combined heat and power configurations have not been studied in depth, as the heat requirements of offshore installations are often ignored. The few studies considering the issue focused on steam Rankine cycles [12], [21], [22], while the potential of an ORC bottoming cycle in a cogenerative mode was relatively unexplored. Second, the vast majority of the studies were based on case studies making the obtained outcomes case-specific and difficult to generalize. Such approach is limiting when assessing the feasibility of a technology for a given application, especially when a large range of working conditions are possible as it is the case for offshore oil and gas platforms. The present work addresses both gaps giving a novel contribution to the field of study. To the best of the authors' knowledge, there is no other scientific work that deals with offshore power and heat production from gas turbines waste heat by means of an ORC and that considers a wide spectrum of facility heat loads and varying exhaust gas temperatures. The main aim of the present study is to investigate the most efficient opportunities of waste heat recovery from the offshore gas turbine exhaust gas and to provide guidelines on the optimal approaches to combined heat and power production based on the characteristics of offshore installations. Since no standard configuration exists, two different layouts are presented and compared from the viewpoint of exergy. These configurations were based on the idea of power generation followed by heat production and vice versa, namely cascade and series systems, respectively. Effects on the system exergetic performance of different working fluids were investigated. In addition, results were compared for the series system with simple and recuperated ORC, considering two condenser pressure levels.

Furthermore, the distribution of exergy destruction within the system components operating with the most appropriate working fluid was obtained under the specified conditions.

2. Systems description and assumptions

2.1.System description

The cogeneration systems considered in this study are shown schematically in Figs. 1 and 2. The heat demand of the generic offshore facility was assumed to be at two temperature levels (described in detail in the following subsection). Therefore, heat recovery from the gas turbine exhaust gas occurred at two different stages. In the cascade configuration shown in Fig. 1, the power generation is followed by heat production. Ideally, this is the most efficient layout from an exergy viewpoint. As shown, the gas turbine exhaust gas is first utilized in the ORC evaporator (EVA) to run the ORC and generate mechanical power. The remaining available thermal energy of the exhaust gas is then used in Heat Exchanger 2 (HEX2) to produce high temperature heat. The organic working fluid evaporates before expanding in the ORC turbine (ORCT). Next, it enters Heat Exchanger 1 (HEX1) and is cooled to the saturated liquid by delivering heat to the heat transfer fluid. HEX1 acts as a condenser for the ORC and as a heat source to produce the low temperature process heat. The heat transfer fluid absorbs heat from the ORC working fluid in HEX1 and supplies it to the low temperature processes (LTP). Similarly, heat transfer fluid is heated in HEX2 to the appropriate temperature for high temperature processes (HTP).

In the configuration shown in Fig. 2, power generation follows after heat production. Here, the heat recovered from exhaust gas first produces the high temperature heat in HEX1, and then the low temperature heat in HEX2, and finally the power. The exhaust gas is cooled to the minimum allowed temperature in the evaporator (EVA) and evaporates the ORC working fluid to run the

ORC turbine. The expanded organic fluid is cooled to saturated liquid state in the ORC condenser before flowing to the pump (ORCP). Pressurized working fluid then enters the evaporator and completes the cycle.

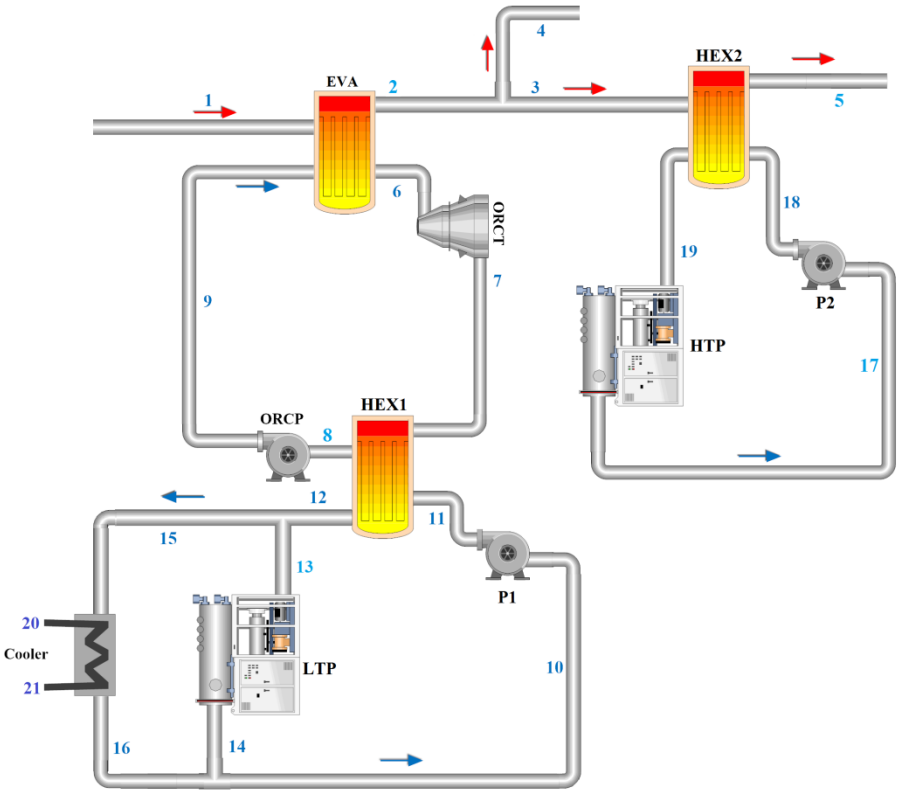

Fig. 1 Schematic diagram of the proposed cogeneration cascade system

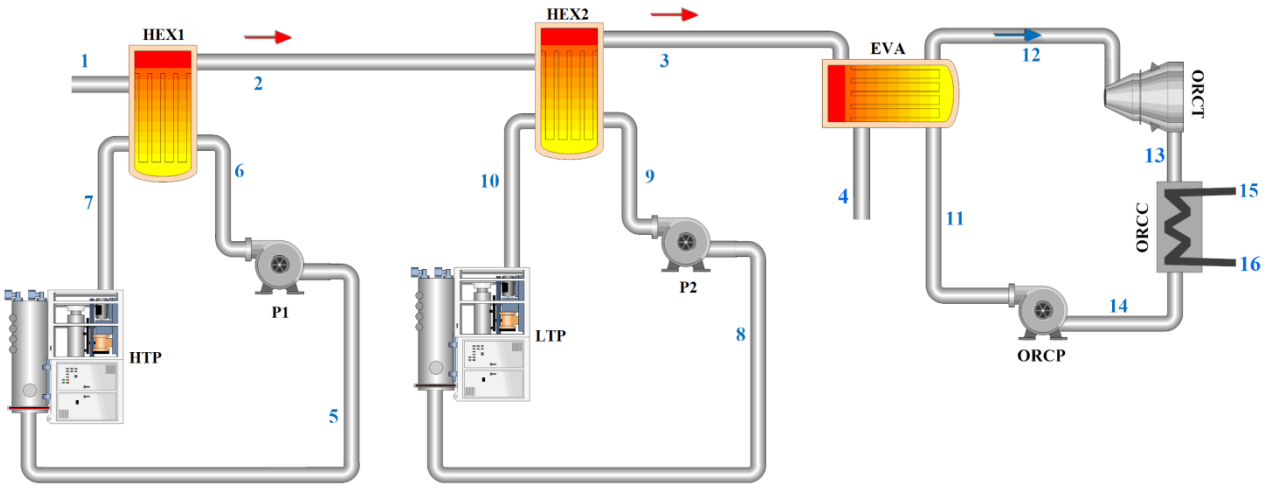

Fig. 2 Schematic diagram of the proposed cogeneration series system

2.2.Analysis framework

To allow for more general results, a large range of realistic cases were assessed rather than a specific case study. Two parameters were varied to define the different cases:

- The temperature of the gas turbine exhaust gas
- The overall heat requirement of the offshore installation

With respect to the exhaust gas temperature, four values were considered (375 °C, 450 °C, 525 °C and 600 °C). The values selected did not necessarily represent any existing gas turbine, but aimed to represent the range of gas turbine models relevant for offshore applications. A selection of gas turbines currently used offshore, with design and performance data at specified ambient conditions, can be found in [20]. Similarly, the heat requirement was varied to encompass different scenarios representing offshore plants with different characteristics or in different stages of field exploitation. Five values were considered, ranging from 5 MW to 25 MW with

intervals of 5 MW. This was in line with the typical heat demands reported in the literature. The combinations of exhaust gas temperature and overall heat requirement defined the generic cases to be assessed.

Other parameters were kept constant in the first instance, in order to limit the number of cases to be tested. Assuming that an offshore installation requires heat at different temperature levels, the temperature levels and the shares between them should be defined. The choice of the related values was important to define the scope of the analysis. The values assumed should be reasonable within the field of selected application to generalize the obtained results. Based on the relevant literature, the largest heat consumer is the crude oil separation process involving heating of oil to temperatures between 50 and 90 °C [8], [21], [23]. Other units may need heat at low temperature (e.g. fuel gas heating), but their heat requirements are relatively small [23]. Furthermore, heat is also requested at relatively high temperatures, e.g. gas dehydration with the reboiler operating at around 200 °C [24] or oil stabilization with the reboiler operating at 180-200 °C [23]. In addition, other plants pertinent to the field of application under investigation, such as liquefied natural gas plants [25] or natural gas processing plants [26], could include processes demanding heat at similar, if not higher, temperature levels. The share of the overall heat demand requested by these processes is normally a smaller fraction of the total. Given the overview presented, the following values were assigned to the parameters, in order to set a realistic analysis framework:

- Low and high temperature levels at 150 and 250 ˚C, respectively.
- Heat at low and high temperature levels at 90% and 10%, respectively, of the total heat requirement.

Furthermore, in order to simplify the simulations, the following choices and assumptions were adopted in this study:

- The whole system operated under steady state conditions.
- Ambient temperature and pressure at 10 ˚C and 1.013 bar, respectively, which are representative conditions for the North Sea [4], [27].
- The temperature of exhaust gas released to the atmosphere was limited downwards to 145 ˚C to prevent condensation of corrosive compounds [28] (e.g. nitric acid from NOx).
- A mass flow rate of 85 kg/s for the exhaust gas, which is in line with the gas turbine models used offshore [20].
- The exhaust gas composition calculated assuming complete combustion [29].
- Pressure losses of 3% for the liquid side and 25 mbar for the gas side of heat exchangers, while pressure losses along pipelines were neglected.
- A minimum temperature difference of 10 ˚C in all heat exchangers.
- The maximum pressures in the ORC limited to 95% of working fluid critical pressure. Based on previous studies, supercritical ORCs was not a mature technology compared with subcritical ones. The high cost and low efficiency of multistage pumps required for transcritical ORCs was one of the main reasons why these cycles were not widely adopted [30].
- The ORC condenser pressure constrained to be above the atmospheric pressure [31]. The reason for this was that employing devices to remove non-condensable gases (in vacuum cases) increases the complexity of the waste heat recovery system, which is not favorable in offshore applications.
- Pumps and turbines had isentropic efficiencies of 75% and 85%, respectively.

- The ORC pump inlet flow is saturated liquid.
- Heat losses from the system components and pipelines were insignificant.

Dowtherm-A was used as heat transfer fluid, which has pressure drops of 1 bar during low and high temperature processes. Its thermophysical properties are outlined in Table 1, while Table 2 lists those of the organic working fluids. The table presents properties of three siloxanes (D5, MM and MDM) and two refrigerants (R123 and R124), which were used in the simulations. It should be noted that the use of R123 and R124 will be banned by the Montreal protocol. However, these refrigerants are utilized as working fluids for ORCs in a wide variety of previous studies [32]–[35], and they are employed here for comparison with siloxanes, which are known as suitable working fluids for high temperature ORCs. A minimum temperature of 20 ˚C is considered for the refrigerants as working fluid. Furthermore, the exhaust gas specific heats were modeled according to McBride et al. [36].

Table 1

Thermodynamic properties of Dowtherm-A as the selected heat transfer fluid [20], [37].

Molecular weight (kg/kmol)	Critical temperature (˚C)	Critical pressure (bar)	Freezing temperature at 1 atm (°C)	Density at 25 °C (kg/m^3)	Vapor pressure at 330 °C (bar)
166	497	31.34	12	1056	3.96

Table 2

Thermodynamic properties of the organic working fluids used in the ORC [38]–[42].

Compound	Molecular weight (kg/kmol)	Critical temperature (˚C)	Critical pressure (bar)	Boiling temperature at 1 atm (°C)	Eccentric Factor
D5	370.8	346	11.6	209.2	0.6363

MDM	236.5	290.9	14.15	152.6	0.5301
MM	162.4	245.5	19.39	100.3	0.4192
R123	152.9	183.7	36.7	27.8	0.2821
R124	136.5	122.3	36.2	-12.2	0.2861

3. Thermodynamic principles

3.1.Energy analysis

Considering each component of the proposed configurations as a control volume and ignoring the kinetic and potential energies variation, the energy conservation equation under steady state conditions can be written [43] as

$$\dot{Q} - \dot{W} = \sum \dot{m}_e h_e - \sum \dot{m}_i h_i \quad (1)$$

where $\dot{Q}$, $\dot{W}$, $\dot{m}$, and h are rate of heat, mechanical power, mass flow rate and specific enthalpy, respectively. Subscripts *e* and *i* denote exiting and inlet flows, respectively.

Table 3 outlines the applied energy balance equations for the subsystems of both configurations in this study.

Table 3

Energy conservation equations

Component	Equation
Cascade system:	
EVA	$\dot{Q}_{Eva} = \dot{m}_1(h_1 - h_2) = \dot{m}_9(h_6 - h_9)$
ORCT	$\dot{W}_{ORCT} = \dot{m}_6(h_6 - h_7)$, $\eta_{is,ORCT} = \frac{\dot{W}_{ORCT}}{\dot{W}_{is,ORCT}}$

HEX1 $\dot{Q}_{HE1} = \dot{m}_7(h_7 - h_8) = \dot{m}_{11}(h_{12} - h_{11})$

ORCP $\dot{W}_{ORCP} = \dot{m}_8(h_9 - h_8)$, $\eta_{is,ORCP} = \dfrac{\dot{W}_{is,ORCP}}{\dot{W}_{ORCP}}$

P1 $\dot{W}_{P1} = \dot{m}_{10}(h_{11} - h_{10})$, $\eta_{is,P1} = \dfrac{\dot{W}_{is,P1}}{\dot{W}_{P1}}$

LTP $\dot{Q}_{LTP} = \dot{m}_{13}(h_{13} - h_{14})$

Cooler $\dot{Q}_{Cooler} = \dot{m}_{15}(h_{15} - h_{16}) = \dot{m}_{20}(h_{21} - h_{20})$

HE2 $\dot{Q}_{HE2} = \dot{m}_3(h_3 - h_5) = \dot{m}_{18}(h_{19} - h_{18})$

P2 $\dot{W}_{P2} = \dot{m}_{17}(h_{18} - h_{17})$, $\eta_{is,P2} = \dfrac{\dot{W}_{is,P2}}{\dot{W}_{P2}}$

HTP $\dot{Q}_{HTP} = \dot{m}_{19}(h_{19} - h_{17})$

Series system:

HE1 $\dot{Q}_{HE1} = \dot{m}_1(h_1 - h_2) = \dot{m}_6(h_7 - h_6)$

P1 $\dot{W}_{P1} = \dot{m}_5(h_6 - h_5)$, $\eta_{is,P1} = \dfrac{\dot{W}_{is,P1}}{\dot{W}_{P1}}$

HTP $\dot{Q}_{HTP} = \dot{m}_7(h_7 - h_5)$

HE2 $\dot{Q}_{HE2} = \dot{m}_2(h_2 - h_3) = \dot{m}_9(h_{10} - h_9)$

P2 $\dot{W}_{P2} = \dot{m}_8(h_9 - h_8)$, $\eta_{is,P2} = \dfrac{\dot{W}_{is,P2}}{\dot{W}_{P2}}$

LTP $\dot{Q}_{LTP} = \dot{m}_{10}(h_{10} - h_8)$

EVA $\dot{Q}_{Eva} = \dot{m}_3(h_3 - h_4) = \dot{m}_{11}(h_{12} - h_{11})$

ORCT $\dot{W}_{ORCT} = \dot{m}_{12}(h_{12} - h_{13})$, $\eta_{is,ORCT} = \dfrac{\dot{W}_{ORCT}}{\dot{W}_{is,ORCT}}$

ORCC $\dot{Q}_{ORCC} = \dot{m}_{13}(h_{13} - h_{14}) = \dot{m}_{15}(h_{16} - h_{15})$

ORCP	$\dot{W}_{ORCP} = \dot{m}_{14}(h_{11} - h_{14})$, $\eta_{is,ORCP} = \dfrac{\dot{W}_{is,ORCP}}{\dot{W}_{ORCP}}$

3.2.Exergy analysis

Exergy can be defined as the maximum theoretical useful work achievable from the combination of a system and its environment, bringing the system into complete thermodynamic equilibrium with the environment when there is interaction only between the system and the environment [44]. For a comprehensive introduction to the exergy principle, it is referred to textbooks of Kotas [45], Moran et al. [46] or Szargut et al. [44]. Given that each component is considered as a control volume in steady state, the exergy balance equation can be expressed [47] as

$$\sum_{in} \dot{E}_i = \sum_{out} \dot{E}_j + \dot{E}_D \tag{2}$$

Here, $\sum_{in} \dot{E}_i$, $\sum_{out} \dot{E}_j$ and $\dot{E}_D$ are the inlet exergy streams, the useful outlet exergy streams and the exergy destruction associated with the components, respectively. A part of the exergy destruction is due to component internal irreversibilities, while some can be the exergy discharged to the environment (e.g., coolant) without any usage.

The specific physical (a.k.a. thermomechanical) exergy of a stream is a function of the ambient conditions as well as the stream temperature and pressure and can be written as

$$e_i = h_i - h_0 - T_0(s_i - s_0) \tag{3}$$

while the exergy rate of each stream can be accounted as

$$\dot{E}_i = \dot{m}_i e_i \tag{4}$$

In the present work, changes of composition did not occur. Therefore, chemical exergy was not considered.

In order to give a clear understanding of exergy destruction and exergy efficiency, defining the fuel and product for each component is convenient [29]. The desired exergetic output from a component is the product, while the consumed exergy to generate the product is the fuel. Exergy efficiency and destruction can be expressed as

$$\varepsilon = \frac{\dot{E}_P}{\dot{E}_F} \tag{5}$$

and

$$\dot{E}_D = \dot{E}_F - \dot{E}_P \tag{6}$$

In the latter expression, destruction also included the non-utilized discharges to the environment, i.e. the exergy destruction by mixing into the environment specifically associated with the process.

Fuel and product definitions for the components of each system are listed in Table 4 [29].

Table 4

Exergy analysis equations

Components	Fuel	Product
Cascade system:		
EVA	$\dot{E}_1 - \dot{E}_2$	$\dot{E}_6 - \dot{E}_9$

ORCT	$\dot{E}_6 - \dot{E}_7$	$\dot{W}_{ORCT}$
HEX1	$\dot{E}_7 - \dot{E}_8$	$\dot{E}_{12} - \dot{E}_{11}$
ORCP	$\dot{W}_{ORCP}$	$\dot{E}_9 - \dot{E}_8$
P1	$\dot{W}_{P1}$	$\dot{E}_{11} - \dot{E}_{10}$
HE2	$\dot{E}_3 - \dot{E}_5$	$\dot{E}_{19} - \dot{E}_{18}$
P2	$\dot{W}_{P2}$	$\dot{E}_{18} - \dot{E}_{17}$
Series system:		
HE1	$\dot{E}_1 - \dot{E}_2$	$\dot{E}_7 - \dot{E}_6$
P1	$\dot{W}_{P1}$	$\dot{E}_6 - \dot{E}_5$
HE2	$\dot{E}_2 - \dot{E}_3$	$\dot{E}_{10} - \dot{E}_9$
P2	$\dot{W}_{P1}$	$\dot{E}_9 - \dot{E}_8$
EVA	$\dot{E}_3 - \dot{E}_4$	$\dot{E}_{12} - \dot{E}_{11}$
ORCT	$\dot{E}_{12} - \dot{E}_{13}$	$\dot{W}_{ORCT}$
ORCP	$\dot{W}_{ORCP}$	$\dot{E}_{22} - \dot{E}_{23}$

3.3.Exergy efficiency

The exergetic or second law efficiency of the considered systems and subsystems can be defined as the fraction of supplied fuel exergy that can be found in the product. Accordingly, the exergy efficiency of the overall systems was the rate of exergy of the produced heat and the generated net power divided by the exergy of the exhaust gas entering the system.

This can be expressed for the cascade system as

$$\varepsilon = \frac{\dot{E}_{13} - \dot{E}_{14} + \dot{E}_{19} - \dot{E}_{17} + \dot{W}_{ORCT} - \dot{W}_{ORCP} - \dot{W}_{P1} - \dot{W}_{P1}}{\dot{E}_1} \quad (7)$$

and for the series system as

$$\varepsilon = \frac{\dot{E}_7 - \dot{E}_5 + \dot{E}_{10} - \dot{E}_8 + \dot{W}_{ORCT} - \dot{W}_{ORCP} - \dot{W}_{P1} - \dot{W}_{P1}}{\dot{E}_1} \quad (8)$$

4. Results and discussions

4.1.Available energy and exergy

Before reporting the simulation results, the thermal energy and thermomechanical exergy of the gas turbines exhaust gas were calculated to show the energy and exergy that can be harvested by the presented waste heat recovery systems. Here, the available energy and exergy refer to the difference between energy and exergy of the gas corresponding to the source and ambient temperatures. Table 5 lists these values for different gas temperatures. In addition, the extractable thermal energy and thermomechanical exergy are included, which indicate the difference between energy and exergy of gas corresponding to the source and allowed minimum stack temperatures.

Table 5

Energy and exergy of the exhaust gas

Exhaust gas temperature (˚C)	375	450	525	600
Available thermal energy (kW)	33622	40867	48235	55723
Available thermomechanical exergy (kW)	12644	16895	21518	26466
Extractable thermal energy (kW)	21468	28714	36082	43569
Extractable thermomechanical exergy (kW)	8579	14153	18776	23724

4.2.Cascade system

For different values of the heat demand (produced heat via system) and gas turbine exhaust temperatures (State 1), as well as different working fluids, the exergetic efficiency and net produced power were computed.

The effects of the heat demand variation on the exergy efficiency and net produced power of the cascade system are shown in Figs. 3-6 for different source temperatures. Here and in subsequent graphs, the simulated cases are represented by symbols. The lines are drawn between the symbols to assist reading and do not represent continuous series of simulations. Whenever the heat demand could not be met by the system, the maximum achievable heat is reported instead. As presented in Fig. 1, the first step in the waste heat recovery is the power generation by the ORC, while the heat rejection from the ORC is utilized for low temperature heating. Therefore, the condensation temperature of the working fluid in HEX1 was set to be higher than that required for the low temperature process. However, it should be noted that the saturation temperature corresponding to the atmospheric pressure (near the ORC minimum pressure) was higher than the specified heating temperature in the cases of D5 and MDM. The critical temperature for the refrigerant R124 was lower than the considered temperature for the low temperature heat demand. Therefore, it was not used as a working fluid in the cascade system.

Referring to Figs. 3-6, the power produced by the ORC was constant while the heat demand changed. The hot gas leaving the evaporator was used to heat the heat transfer fluid to a specific temperature to produce the high temperature heat (10% of the total heat demand). As a result, State 2 in the cascade system had a fixed temperature for all values of heat demand, which explains the constant values of ORC output power. Among the working fluids tested, the highest

condensation pressure belongs to R123, namely 18.5 bar. As the slope of the vapor saturation line of R123 in a *T-s* diagram is negative (wet fluid), the state at the inlet of the turbine should be superheated to avoid condensation during the expansion. Fig. 7 presents the optimum value of superheating degrees corresponding to the maximum net produced power. Superheating the ORC turbine inlet flow increased the enthalpy of the stream and decreased the evaporated working fluid mass flow rate. A tradeoff between these two parameters emerged as the turbine output power was maximized for a certain value of superheating degree. The results associated with R123 are reported considering the optimal superheating degree. However, this working fluid had the largest evaporator temperature mismatching (see Fig. 8), which led to the lowest net power output. Next to R123, the lowest net output power pertained to D5, because this working fluid had the highest condensation temperature and the largest HEX1 temperature mismatching. It is worth mentioning that, unlike R123, superheating siloxanes in the ORC turbine inlet flow decreased the turbine output power.

The produced power and total exergy efficiency associated with the MM and MDM were almost the same, namely (for MM/MDM) 858/855, 1431/1425, 2013/2006 and 2605/2595 kW at the source temperatures of 375, 450, 525 and 600 ˚C, respectively. For comparison of MM (or MDM) with D5 as working fluid for this configuration, it was noted that the net produced power and the maximum exergy efficiency for MM were 212, 353, 496 and 643 kW and 1.1, 1.4, 2.3 and 2.4 percentage points higher than those of D5 for the respective source temperatures of 375, 450, 525 and 600 ˚C.

The temperature matching between cold and hot streams in the evaporator and HEX1, or the exergy destruction within these components, explained why the results obtained for MM and MDM were the same. Table 6 presents the values of exergy destruction for the source

temperature of 600 ˚C. It was seen that among the fluids, MM had the second highest exergy destruction in the evaporator, while it had the lowest exergy destruction in HEX1. On the other hand, MDM destroyed more exergy in HEX1 compared with MM, while less in the evaporator. When the combined performance of the evaporator and HEX1 was considered, MM and MDM had approximately the same exergy destruction. It is worth mentioning that here, the available exergy for the evaporator was the same for all working fluids. In addition, a change in the heat load had no effect on the values reported in Table 6. Based on the exergy destruction, the table shows that the order of the best working fluids for the cascade system was MM, MDM, D5 and R123.

Table 6

Exergy destruction within the evaporator and HEX1 of different compounds and a source temperature of 600˚C (all heat loads)

Working fluid	MM	MDM	D5	R123
Destroyed exergy within the evaporator (kW)	6563	5446	3624	7477
Destroyed exergy within HEX1 (kW)	1344	2542	4910	1435
Total destroyed exergy within evaporator and HEX1 (kW)	7907	7988	8534	8912

As Figs. 3 and 4 show, for exhaust temperatures of 375 and 450 ˚C, the cascade system was not able to supply the maximum heat load. The exhaust gas temperatures of 375/450 ˚C gave the maximum produced heat rates associated with MM, MDM, D5 and R123 as 11093/18486, 11096/18492, 11328/18877 and 11554/19254 kW, respectively. In particular, the system was not able to supply the heat load to the low temperature processes.

As shown in Figs. 5 and 6, the thermal energy of the exhaust gas with temperatures of 525 and 600 ˚C were enough to produce the maximum heat demand of 25 MW of heat. Although the temperature profiles in HEX1 and HEX2 were constant, larger rates of heat could be supplied at higher values of the exhaust gas temperature. A higher source temperature led to a higher mass flow rate of working fluid in the evaporator and, as a result, increased the available heat for the heat transfer fluid in HEX1.

When the exhaust gas temperature increased from 375 to 525 ˚C, the exergy efficiency improved mainly due to an increment in the produced heat rate. However, with a further increase of the source temperature to 600 ˚C, the exergy efficiency was reduced for a fixed heat production rate, even though the generated power increased. This was because at a source temperature of 600 ˚C, the mass flow rate of heat transfer fluid was higher than the required value corresponding to the maximum heat load. Then, a part of the heat transfer fluid was cooled in the cooler without participating in heat delivery. For instance, for MM at the maximum heat load and exhaust gas temperatures of 525 and 600 ˚C, the fractions of heat transfer fluid mass flow rates that pass the cooler and waste exergy were 6.6 and 26.8%, respectively.

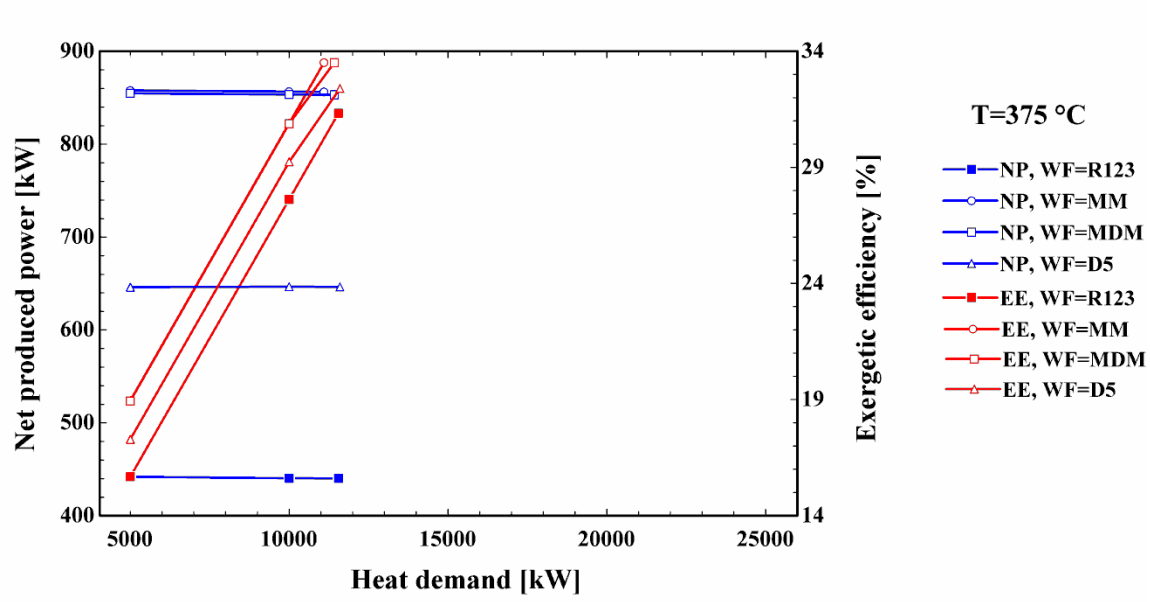

Fig. 3 Net produced power and the exergy efficiency of the cascade system versus the heat demand for a gas turbine exhaust temperature of 375 ˚C

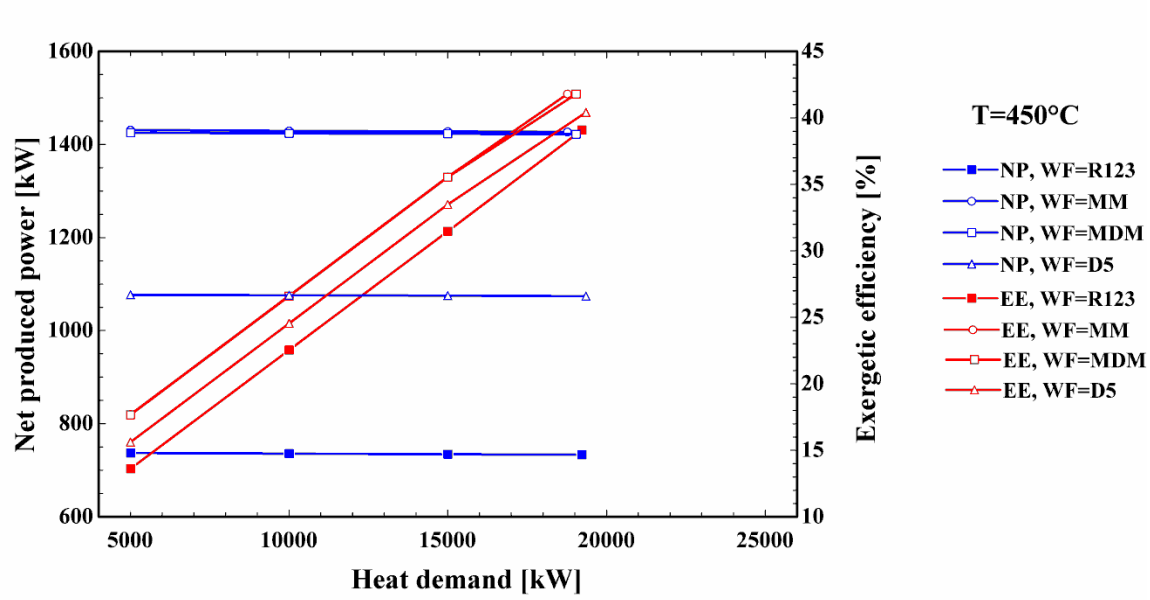

Fig. 4 Net produced power and the exergy efficiency of the cascade system versus the heat demand for a gas turbine exhaust temperature of 450 ˚C

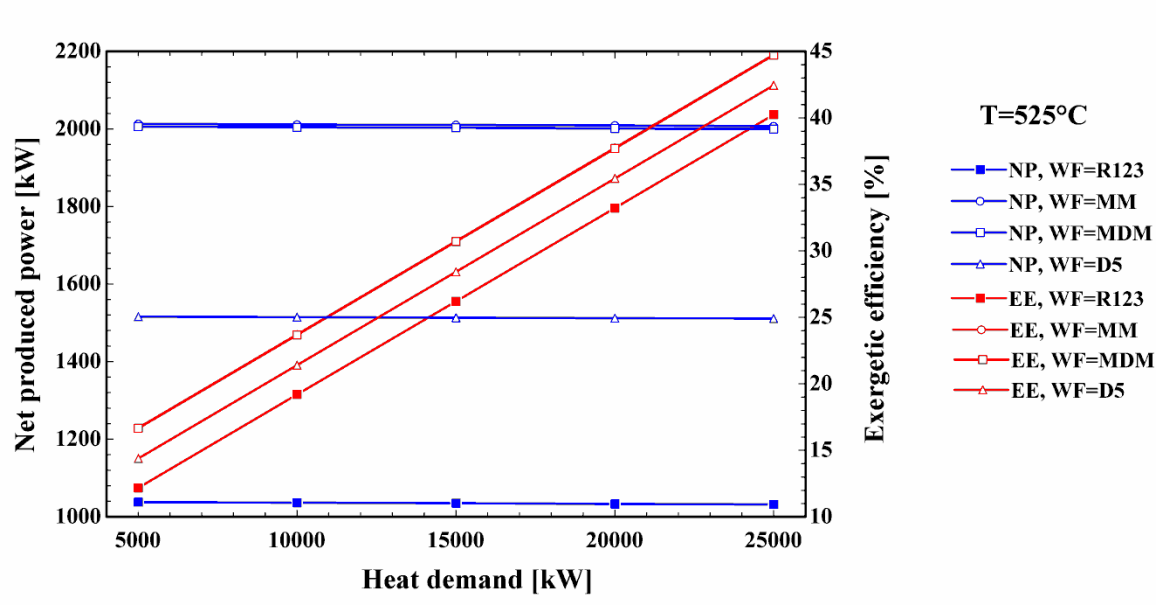

Fig. 5 Net produced power and the exergy efficiency of the cascade system versus the heat demand for a gas turbine exhaust temperature of 525 ˚C (MDM overlaps MM)

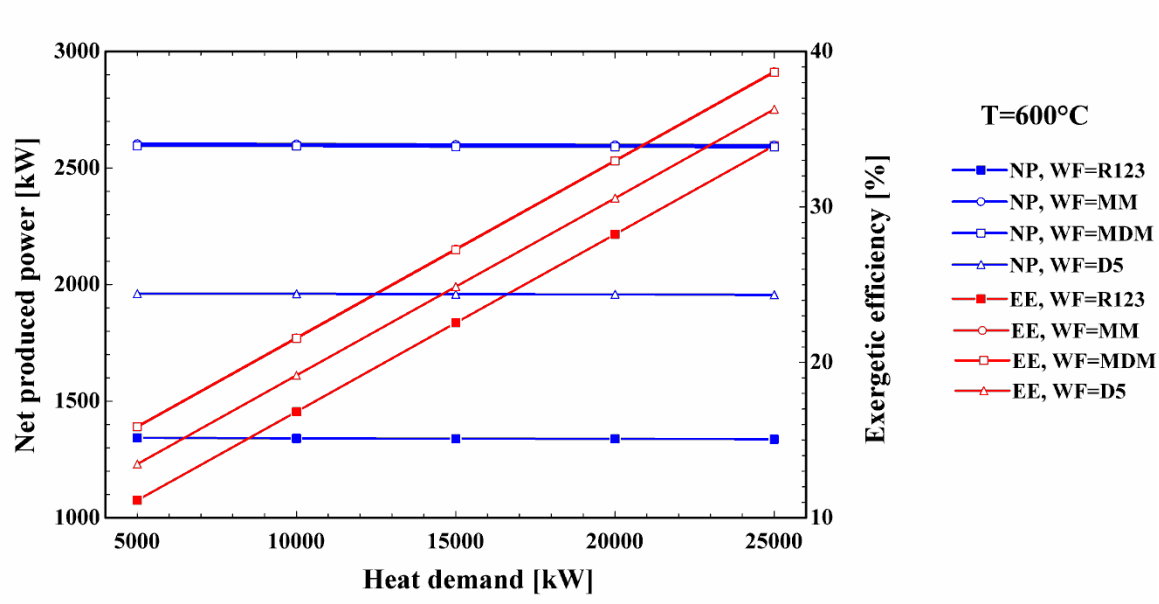

Fig. 6 Net produced power and the exergy efficiency of the cascade system versus the heat demand for a gas turbine exhaust temperature of 600 ˚C (MDM overlaps MM)

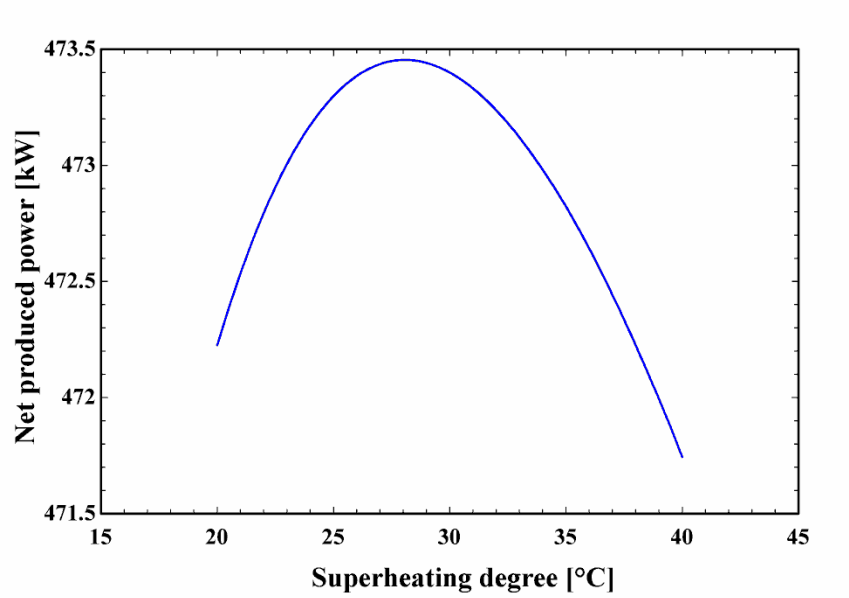

Fig. 7 ORC turbine inlet flow superheating degree versus net produced power for R123 as the working fluid

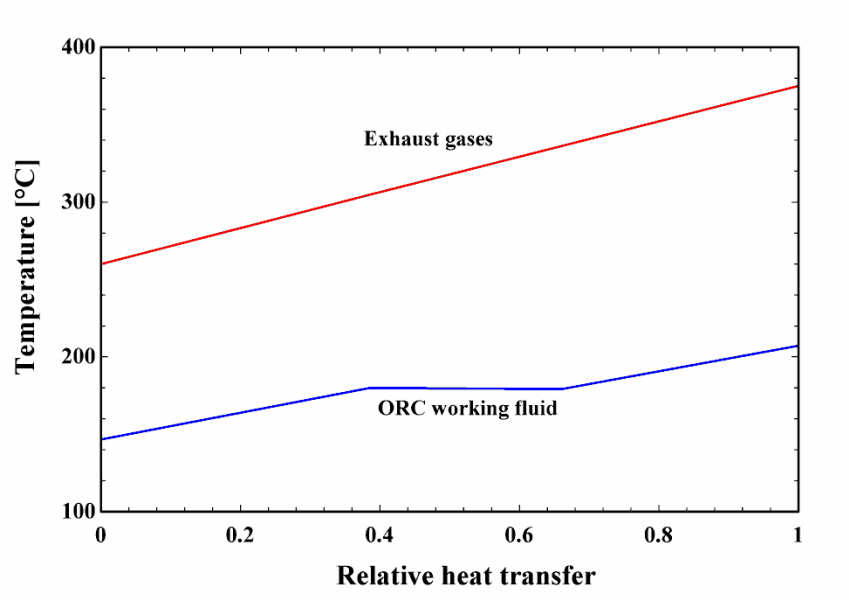

Fig. 8 Temperature versus relative heat transfer in the evaporator for R123 as working fluid and a source temperature of 375 ˚C

Fig. 9 shows the exergy destruction values within the cascade system components as well as effluent exergy (gas released to the environment) under different operating conditions when MM was used as working fluid. For the cooler, the reported values of the exergy destruction represent destroyed exergy within this component as well as the exergy loss, since the exergy rate related

to heated coolant in this component is not used anywhere. As Fig. 9 illustrates, changing the heat load with a constant heat source temperature had no effect on the exergy destruction within the evaporator, ORC pump, HEX1, P1 and ORC turbine. This was because the temperature profiles in the evaporator and HEX1 were fixed, which kept the exergy destruction constant within the mentioned components. At lower heat loads, the most exergy destructive component was the cooler, while at higher heat loads, more exergy destruction occurred in the evaporator. In addition, increasing the heat load reduced the effluent exergy (an exergy loss), since a larger fraction of the evaporator exiting hot gas entered HEX2.

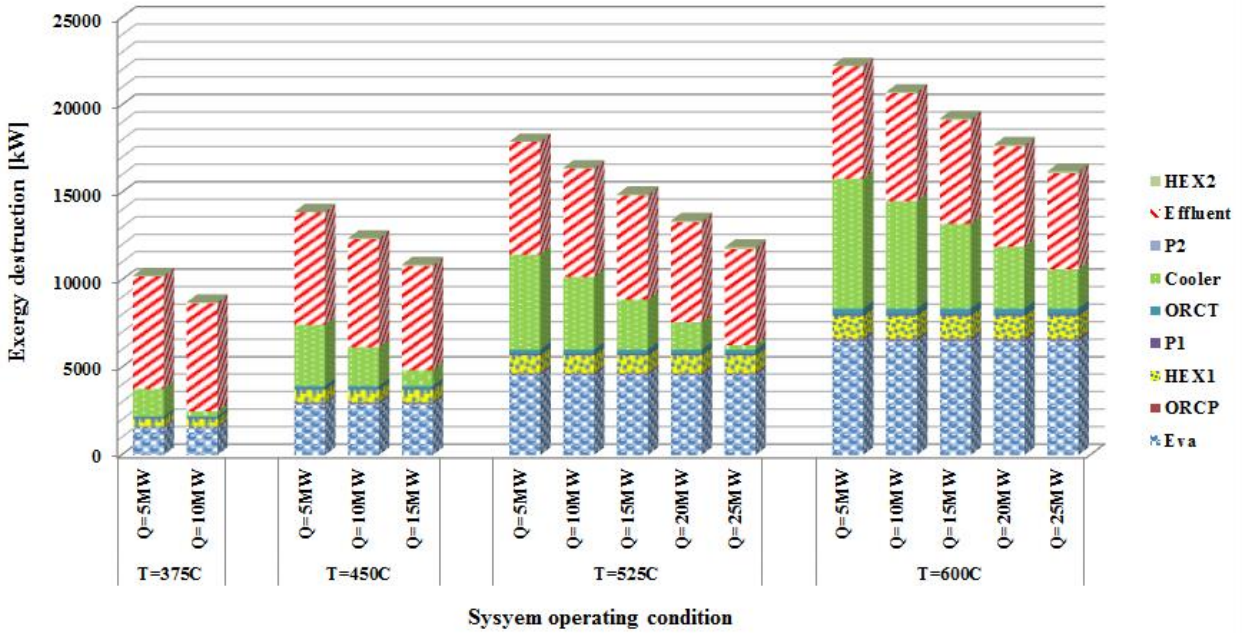

Fig. 9 Exergy destruction within the cascade system components with MM as the ORC working fluid

4.3.Series system

The exergy efficiency and net produced power of the series system under various heat loads and source temperatures are shown in Figs. 10-13. Different from the cascade system, the

temperature profiles in the heat exchangers were not constant in this system and changed with the variation of the source temperature and heat load. In the series system, heat is first transferred to the heat transfer fluids in HEX1 and HEX2, before the ORC utilizes the remaining thermal energy of the exhaust gas. At lower levels of heat source temperature, this could lead to cases where the conversion of the residual waste heat to power by the ORC is practically unfeasible, as seen from the interrupted lines in Figs. 10 and 11. For instance, at a gas temperature of 375 ˚C and a heat load of 15 MW, the flue gas left HEX2 with a temperature (216 ˚C) lower than that needed to run the ORC with D5 as working fluid. Unlike D5, R124 was able to produce extra power in the ORC while the system supplied the requested heat demand, since it has a lower critical temperature. As seen in Table 5, the maximum achievable heat load was 21.5 MW.

According to Figs. 10-13, although an increase in the heat production causes a considerable reduction in the net power output, it also increased the total exergy efficiency significantly. This was because the effect of the produced exergy associated with the heat load was higher than that of the generated power on the total exergy efficiency. The exergy efficiency also improved as the heat production increased because increasing the heat production led to larger temperature drops on the exhaust gas side. In turn, this improved the temperature matching between cold and hot streams in the heat exchangers and the evaporator.

Even though the worst temperature matching and the highest exergy destruction in the evaporator pertained to R124, the highest power generation and exergetic efficiency were found for this working fluid in all cases tested. To explain this, the exergy destruction within both evaporator and ORC condenser should be considered simultaneously. Table 7 presents the exergy destruction in these components for the source temperature of 600 ˚C and maximum heat production (25 MW). R124 gave a lower exergy destruction compared with MM and MDM. For

the case of D5, it should be noted that the evaporator exiting gas had a higher temperature (with respect to that of the other working fluids) because of the higher condensation temperature. The lower exergy made available within the evaporator (5849 kW) in the case of D5 explained why a lower exergy destruction for this working fluid did not correspond to a better exergetic performance and higher power production. It should be kept in mind that since the heated coolant in the ORC condenser had no further usage, the destroyed exergy term of this component included the exergy loss of the discharged coolant.

Table 7

Exergy destruction within the evaporator and the ORC condenser of different working fluids with a source temperature of 600˚C and maximum heat load, series system

Working fluids	MM	MDM	D5	R124
Destroyed exergy within the evaporator (kW)	1515	583	323	4697
Destroyed exergy within the ORC condenser (kW)	4571	5724	4765	601
Total destroyed exergy within evaporator and ORC condenser (kW)	6086	6307	5088	5298

One of the advantages of R124 was that it had a condensing pressure 3.8 times the atmospheric pressure, while the condensing pressures of the other working fluids were constrained to be above atmospheric. It was also evaluated that for R124, an optimum turbine inlet pressure can be found that maximizes the power output (see Fig. 14). The optimum turbine inlet pressure was approximately the same for all the heat source temperatures. Performance of siloxanes improved linearly when increasing the ORC higher pressure, which was limited to be less than 95% of the working fluid critical pressure. In addition, in some cases, limitations arose with respect to the 10 K of pinch point temperature difference in the evaporator.

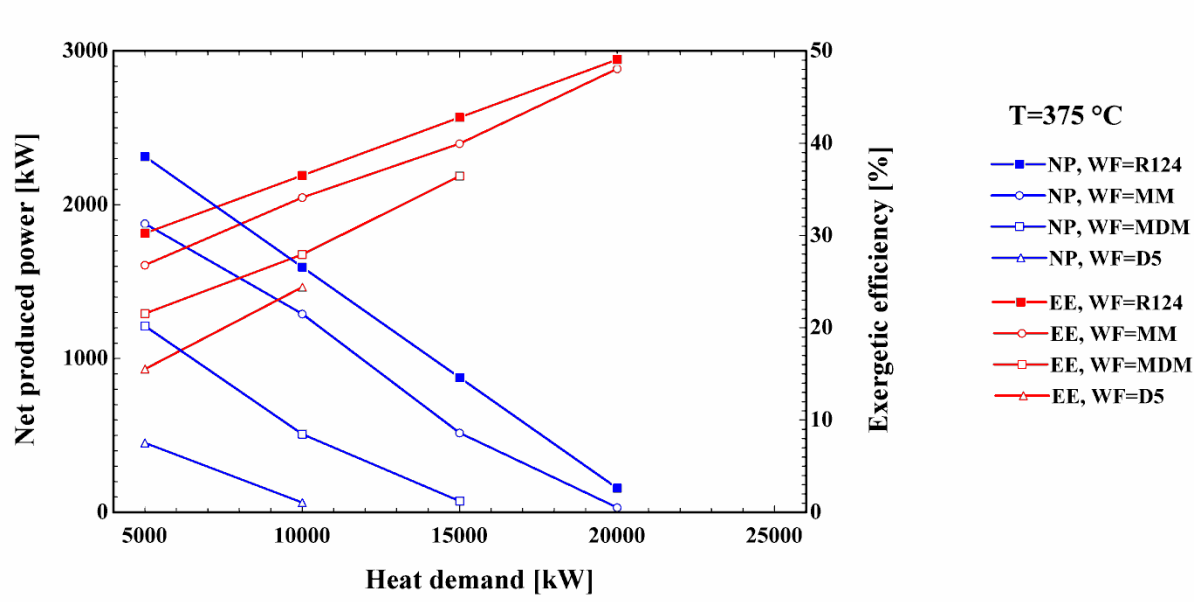

Fig. 10 Effect of the heat requirement on the net produced power and the exergy efficiency of the series system for a gas turbine exhaust temperature of 375 ˚C

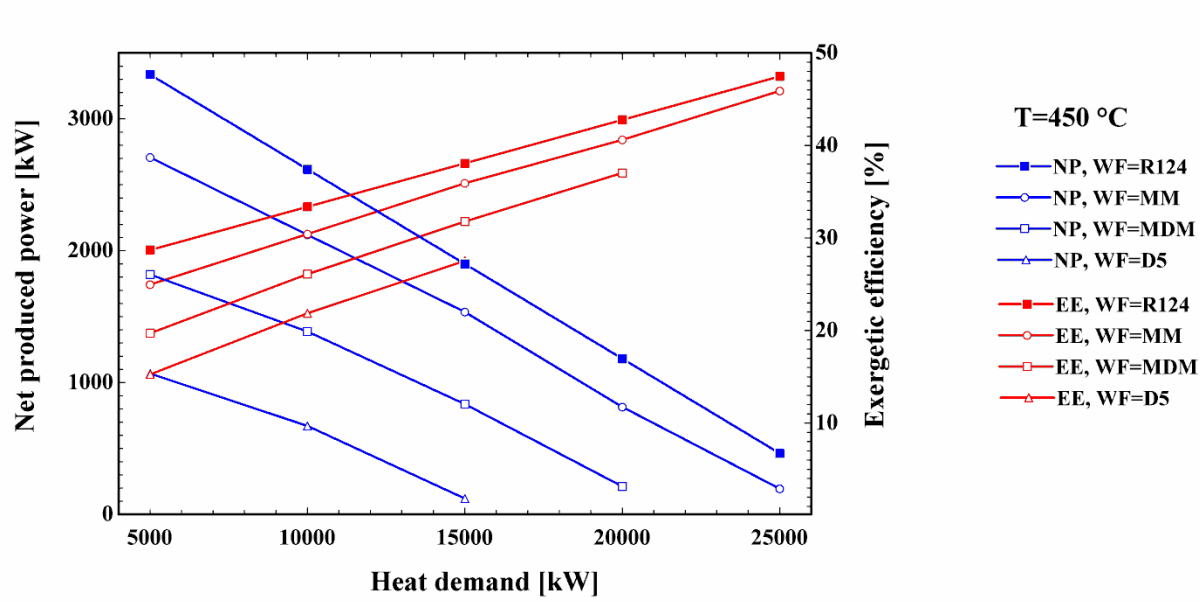

Fig. 11 Effect of the heat requirement on the net produced power and the exergy efficiency of the series system for a gas turbine exhaust temperature of 450 ˚C

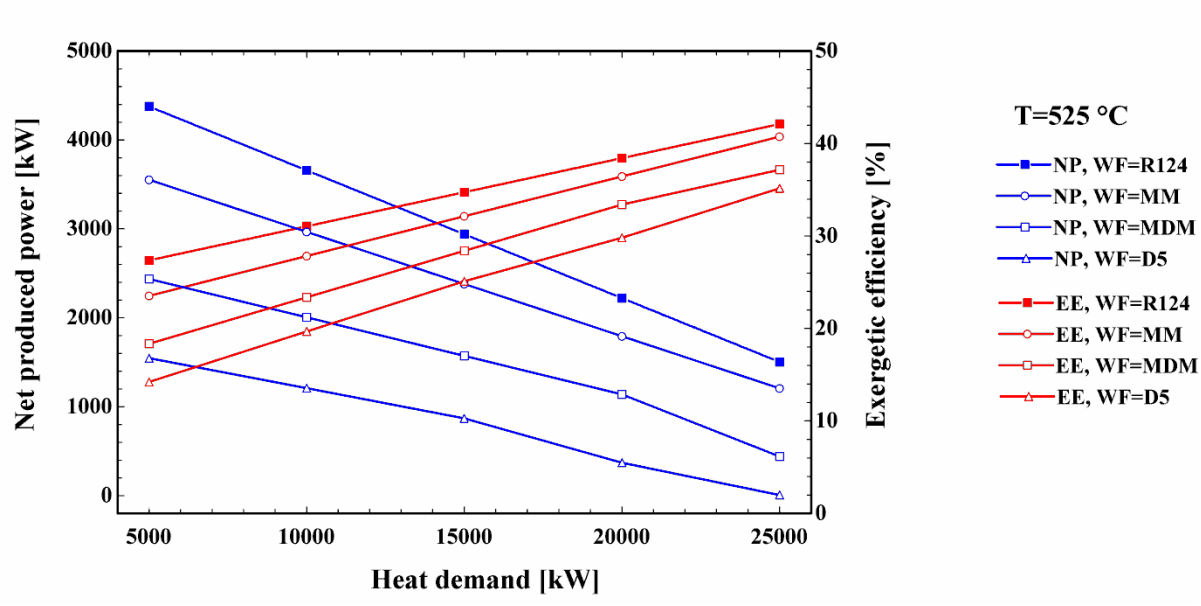

Fig. 12 Effect of the heat requirement on the net produced power and the exergy efficiency of the series system for a gas turbine exhaust temperature of 525 ˚C

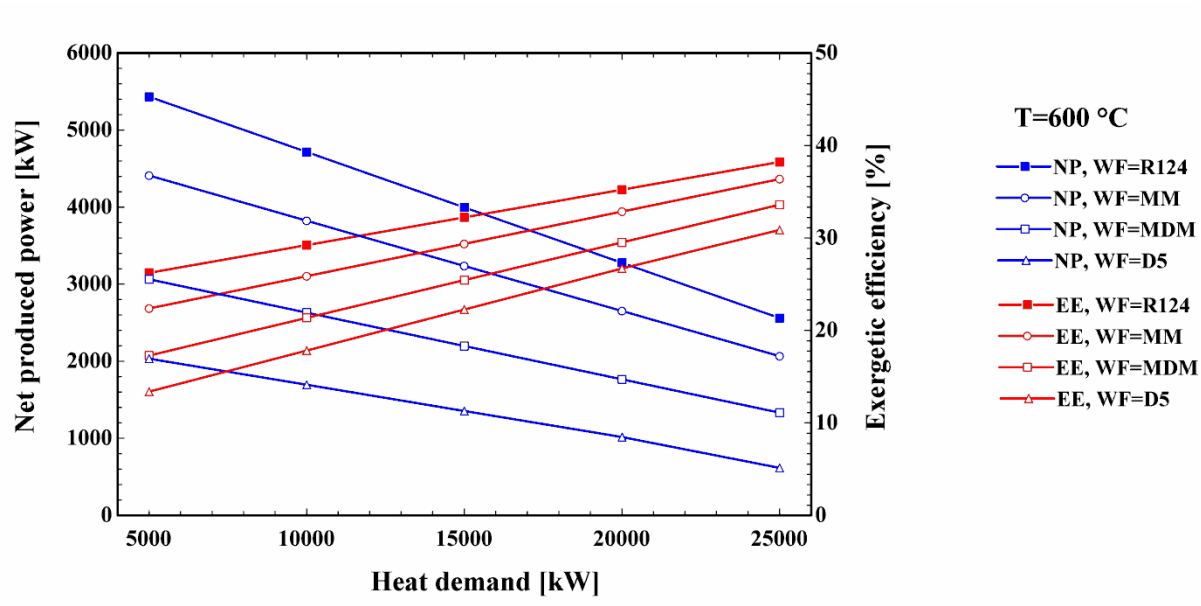

Fig. 13 Effect of the heat requirement on the net produced power and the exergy efficiency of the series system for a gas turbine exhaust temperature of 600 ˚C

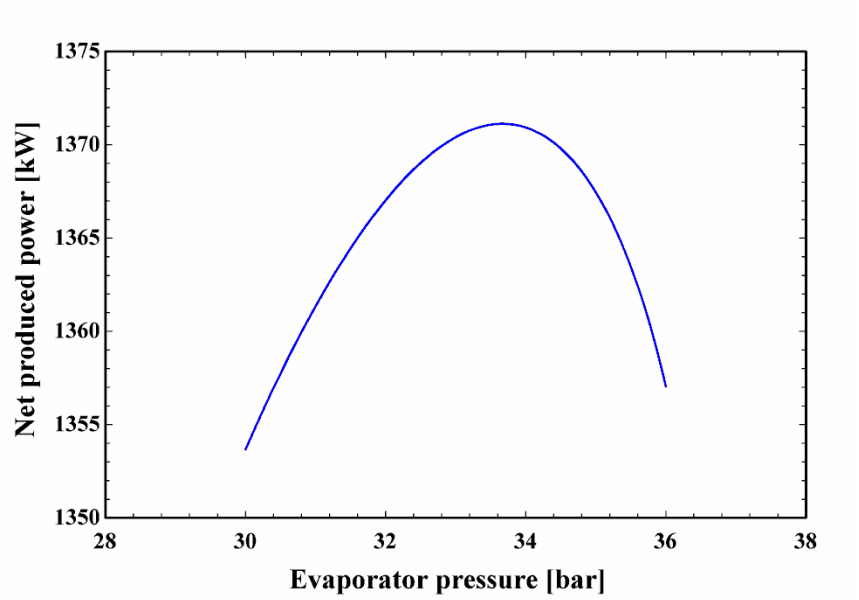

Fig. 14 ORC maximum pressure versus the net produced power for R124 as working fluid and a gas turbine exhaust temperature of 375 ˚C, series system

Exergy destruction within different components of the series system, as well as the effluent exergy (State 4), are shown in Fig. 15 for refrigerant R124 in the series system. It is seen that the most exergy destructive components of the series system vary as a function of heat load. At lower heat loads, the gas stream entering the evaporator had a higher temperature, which resulted in a poorer temperature matching and more exergy destruction. In both HEX1 and HEX2, increasing heat load led to an increase in exergy destruction. In fact, an increase in heat load, although improved temperature profiles within these components, increased the heat transfer fluid mass flow rate and, as a result, the exergy destruction rates. Since the terminal temperature of the exhaust gas was kept constant, the exergy loss associated with the released gas had a constant value in all the conditions evaluated.

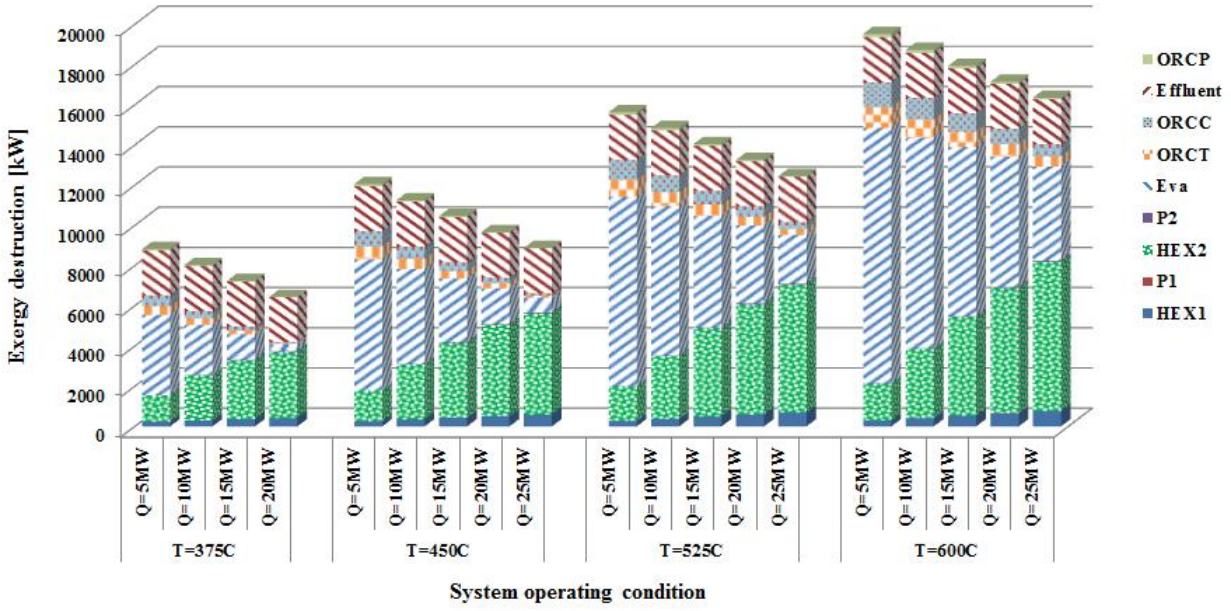

Fig. 15 Exergy destruction within the series system components with R124 as the ORC working fluid

Results associated with both the cascade and series systems are presented, and comparing the two configurations revealed that siloxanes operated better in the cascade system, while refrigerant R124 gave the best results for the series system. In addition, at lower source temperatures, the series system supplied higher heat loads and can be of interest from this point of view. Furthermore, in the cascade system, the exergy destruction in the evaporator (the main exergy destructive component) was constant for each source temperature. In the series system, the destroyed exergy within this component decreased with increasing heat demand.

4.4.Effects of using a recuperator in the series system

As revealed in the previous section, the ORC condenser was the most exergy destructive component of the series system when siloxanes were used in the simulation. With regard to this, it was decided to evaluate the potential benefits of utilizing a recuperator (IHEX) that harvests thermal energy from the ORC turbine outlet flow before the condenser. Drawbacks of

introducing a recuperator are that it increases the complexity of the ORC and the weight and space occupation by the system. Therefore, it was not considered for the base case analyses. A flowsheet of the serial system equipped with recuperated ORC is shown in Fig. 16. The working fluid R124 was not included here because this fluid was wet at the ORC turbine outlet and hence, had no recuperation potential. The effect on the produced net power is illustrated in Fig. 17 for a source temperature of 600 ˚C. It can be seen that at low heat loads, using a recuperator had a remarkable impact on the system performance, while increasing the heat production decreased this influence. This was because higher values of heat load reduced the available thermal energy in the evaporator, which led to a lower flow rate of evaporated working fluid. In turn, this reduced the thermal energy available at the outlet of the ORC turbine and the recuperation potential.

Based on Fig. 17, the recuperated ORC using MM produced more power than the simple ORC using R124. However, the produced power associated with the simple R124 cycle was still higher than that of the recuperated cycles using MDM and D5. It should be pointed out that MDM and D5 had relatively higher condensation temperature, resulting in higher temperature of working fluid entering the evaporator (State 11). Finally, the evaporator exiting gas temperature (State 4) increased and caused a reduction in the extractable energy in the evaporator, which decreased the power.

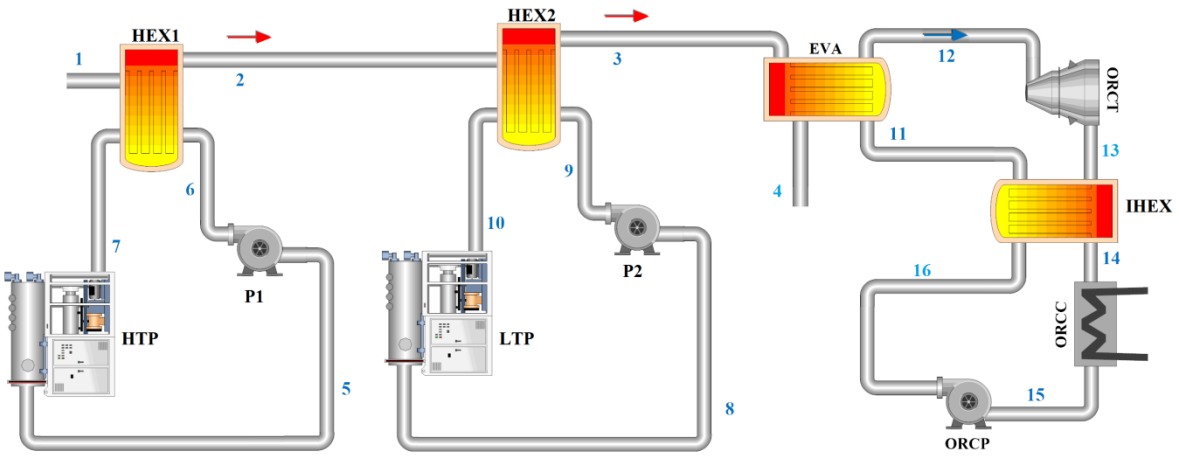

Fig. 16 Schematic diagram of the series waste heat recovery system equipped with recuperated ORC

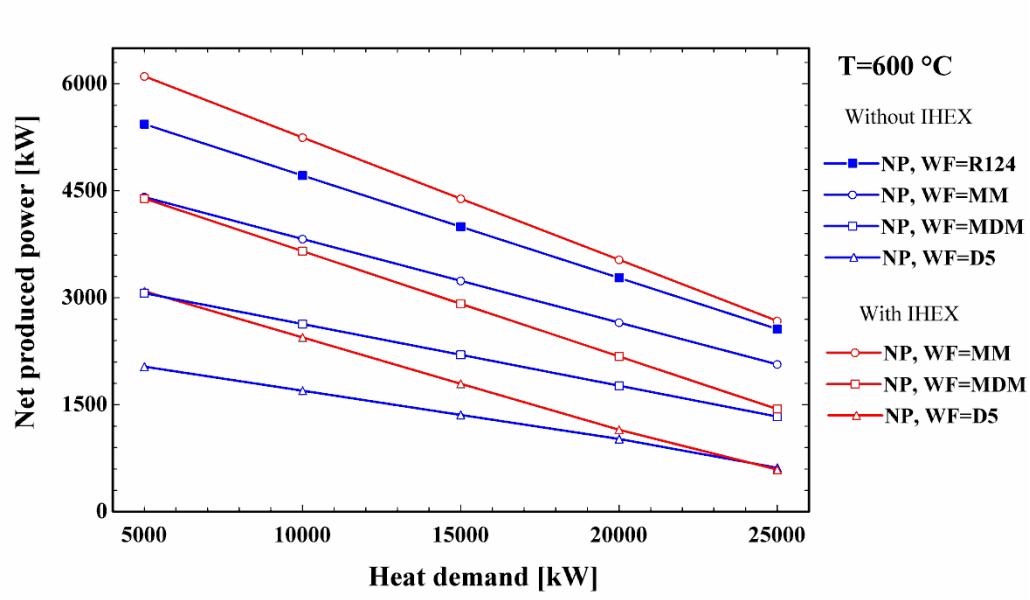

Fig. 17 Effect of using a recuperator (IHEX) on the net output power considering different heat loads and a source temperature of 600˚C

4.5.Effects of reducing ORC minimum pressure (condenser pressure) in the series system

The effects of changing the ORC minimum pressure from above atmospheric (105% of atmospheric pressure) to 5 kPa on the net produced power by the series system were studied in this section, considering both simple and recuperated ORC. For the case of R124, the condenser pressure was 3.8 times the atmospheric pressure, and it was not affected by this sensitivity

analysis. Referring to Fig. 18, decreasing the condenser pressure significantly improved the performance of the ORC when the siloxanes were used as working fluid. As shown in this figure, the effect of reducing condenser pressure was higher than that of employing a recuperator (the minimum condenser pressure at 105% of atmospheric pressure). This was because reducing the ORC minimum pressure not only reduced the exergy destruction in the condenser, but also increased the enthalpy difference between the ORC turbine inlet and outlet, which gave a higher power generation. Comparing Figs. 17 and 18 revealed that MM performed better than R124 in both the recuperated ORC (with superatmospheric condenser pressure) and the simple ORC with a minimum pressure of 5 kPa. Furthermore, recuperated ORC with a condenser pressure of 5 kPa operating with MDM produced more power than the simple ORC using R124, while the simple ORC operating with MDM and minimum pressure of 5 kPa led to a net power comparable with that of the simple ORC using R124. For heat loads lower than 17 MW, the produced power with recuperated ORC and a condenser pressure of 5 kPa operating with D5 was higher than that operating with R124, while vice versa for higher heat loads. In fact, higher heat production reduced the remaining thermal energy for power production, which had a stronger effect on the performance of D5.

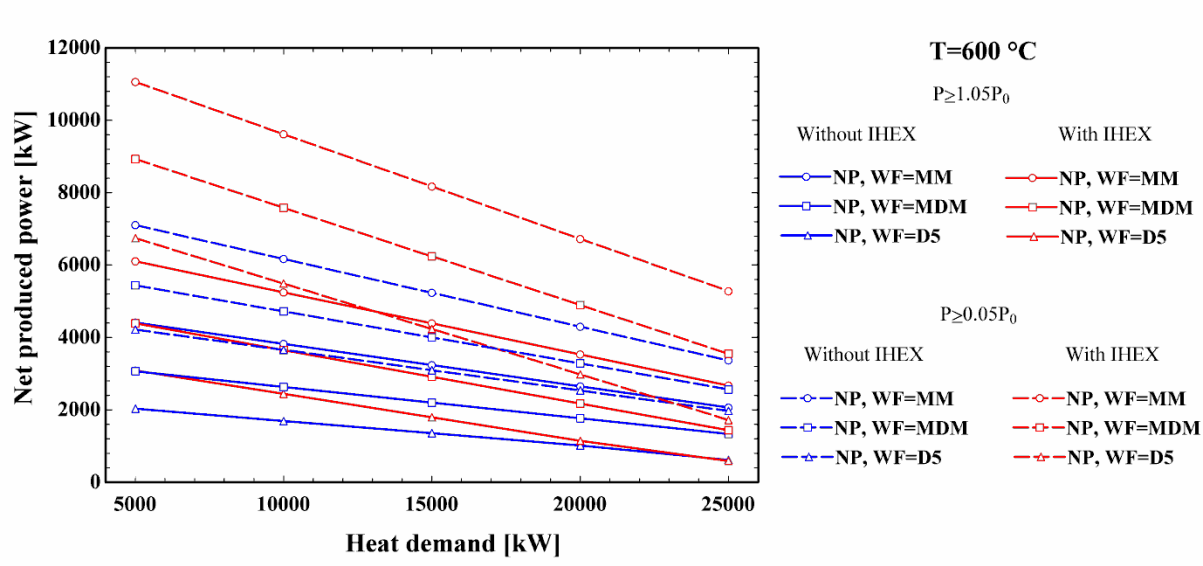

Fig. 18 Effect of using recuperator and decreasing ORC condenser pressure on the net output power when the source temperature was set to 600˚C

The breakdown of the exergy destruction within the series system with recuperated ORC with a condenser pressure of 5 kPa is shown in Fig. 19. The working fluid is MM since it gave the best performance. The trend of the exergy destruction in the different components was similar to that of the series system without recuperator (see Fig. 15).

In order to show the effects of using a recuperator in the series system, as well as reducing the condenser pressure from above atmospheric to 5 kPa in the recuperated ORC, Fig. 20 is presented. All results here are with MM as working fluid and for a source temperature of 600 ˚C. Using a recuperator reduced the exergy destruction in the evaporator and condenser, while increasing the effluent exergy loss and the exergy destruction in the turbine. IHEX performed as a preheater for the working fluid entering the evaporator, thus reducing the associated exergy destruction. In addition, using a recuperator increased the mass flow rate of ORC working fluid and the power output, but it also led to a higher exergy destruction in the ORC turbine. On the

other hand, preheating the working fluid entering the evaporator with a fixed pinch point temperature difference increased the temperature and exergy content of the effluent.

Moving from recuperated ORC with superatmospheric condenser pressure to a recuperative ORC with a condenser pressure of 5 kPa significantly increased the exergy destruction in the evaporator and reduced the exergy destruction in the condenser. This was because using a subatmospheric pressure allowed reduction the condensation temperature. In turn, this reduced the temperature differences within the condenser and the exergy destruction in this component. In addition, reducing the condensation temperature also increased the temperature differences and exergy destruction in the evaporator. Fig. 20 shows that the balance between these contrasting effects was dominated by reduction of exergy destruction in the condenser and that allowing subatmospheric pressures led to lower exergy destruction.

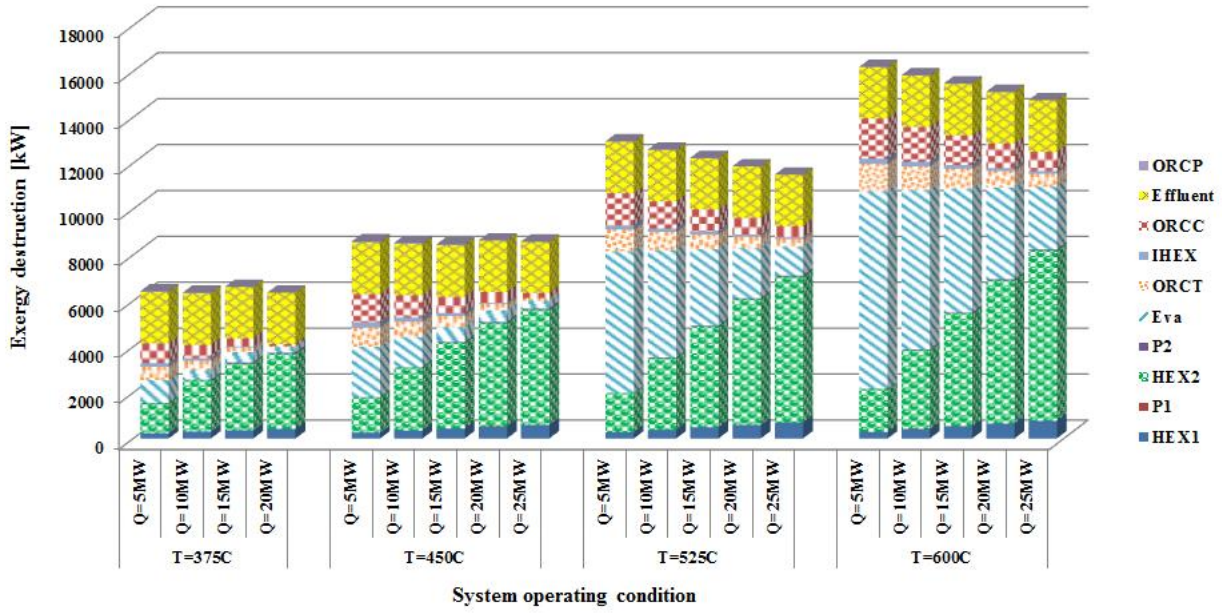

Fig. 19 Exergy destruction within the series system components (equipped with recuperated ORC) with MM as the ORC working fluid

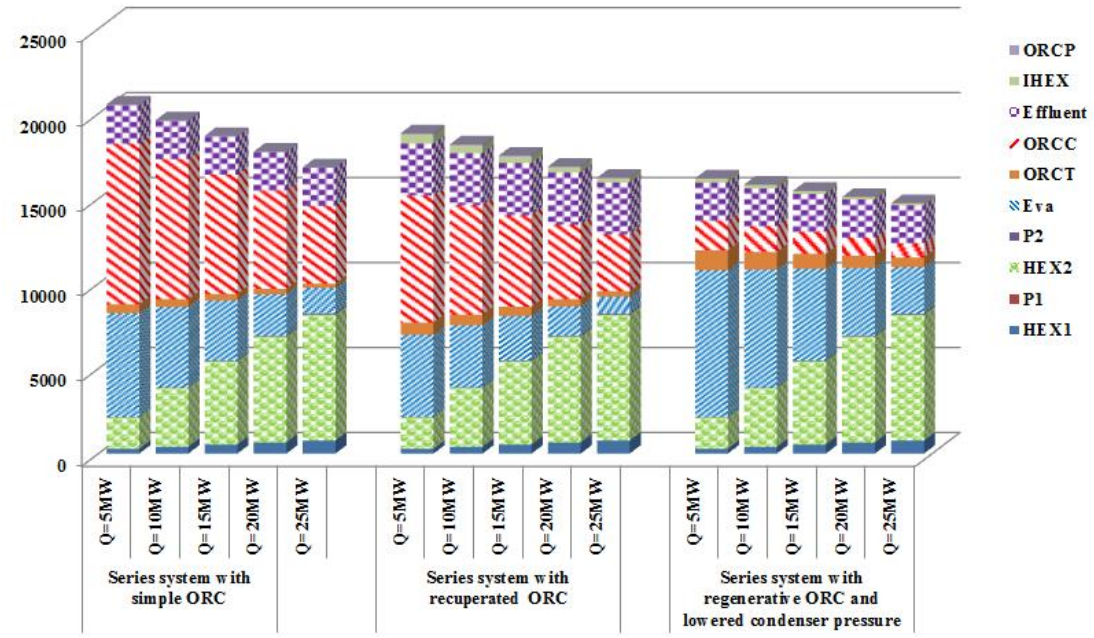

Fig. 20 Exergy destruction versus employing IHEX in the ORC and reducing condenser pressure

4.6.Error Evaluation

Sufficient data for a full error analysis were not available. However, some consideration could still be made. In the simulations, the exhaust gas temperatures and mass flow rate were specified as absolute values. Thus, we regarded these as certain figures. The enthalpy difference for the exhaust gas was modeled with specific heats from the NASA polynomials [36], which for the major species (CO_2, H_2O, N_2, O_2) referred to Gurvič et al. [48], [49]. These sources did not provide uncertainties. However, an earlier survey of data compiled by Touloukian and Makita [50] showed that the deviations were within a range of 0.2-0.3%. Hence, this indicated the magnitude of the relative uncertainties of the heat transferred from exhaust gas to the heating and working fluids.

The propagation of uncertainty from the transferred rate of heat to the produced power can be estimated by the derivative of the latter to the former. Divided by their ratio, the relative error of the power due to heat was (depending on the case) 1-2 times the relative error of the rate of heat.

Compared with more conventional working fluids (e.g. water, CO_2, ammonia), the thermodynamic models of the siloxanes [41], [42] were based on a considerably sparser experimental data. For instance, an uncertainty of isobaric specific heats (and differences of enthalpy and entropy) of D5 was estimated [42] to 25%. This was because the D5 model was based on data for MM as no D5 data were available. For the isothermal differences, including two-phase, an uncertainty of 3% was indicated. The ORC turbine expansion, the enthalpy difference (i.e. the power) can be decomposed into a (negative) isothermal and an isobaric parts. For the D5 cases at exhaust temperature 525 °C, the total expansion enthalpy was 0.35 to 0.55 of the corresponding isobaric component. These figures indicated on the influence of the uncertainty of isobaric specific heats on the power production for D5 cycles, and they will dominate this uncertainty. That is, since the heat transfer is more accurately evaluated, the uncertainties will influence the temperatures more than the power production.

In the comparison of D5 with the other fluids (e.g. Fig. 17), it was seen that the differences were of magnitude 50% or more. Accordingly, although uncertainties were considerable, they did not affect the conclusions regarding appropriateness of the different working fluids.

5. Conclusions

The main findings obtained from the present study were as follows:

- At a fixed source (gas turbine exhaust) temperature, changing heat demand in the cascade system has no effect on the produced power, because heat absorption (evaporator) and

rejection in this system occur at fixed temperature profiles. In the series system, increasing heat load decreases the available thermal energy in the evaporator and significantly reduces the produced power.

- Increasing the heat production leads to an increase in the exergy efficiency of both systems since the produced exergy associated with heat load is higher than that of power production.
- The viability of the cascade system is limited from the viewpoint of heat production for low values of heat source temperature.
- For a fixed value of heat production, increasing the heat source temperature maximizes the exergy efficiency of the cascade system. This is because a source temperature of 525 ˚C is sufficient to produce the maximum heat load. A source temperature of 600 ˚C (as the considered maximum temperature) increases the exergy destruction within this system.
- MM is the best option for the cascade configuration. For the simple series system (without an internal recuperator), R124 operates as the best working fluid.
- The performance of the series system using siloxanes as working fluid (MM, MDM, and D5) increases significantly when using a recuperator, which is due to reducing destroyed exergy within the condenser. MM becomes the best working fluid (instead of R124) for the series system when a recuperator is considered.
- The performance of simple and recuperated ORC using siloxanes significantly increases when subatmospheric condensing pressures are allowed. Adopting subatmospheric pressures increases the exergy destruction in the evaporator and turbine, but it also

reduces the exergy destruction in the condenser. This balance is dominated by the reduction of exergy destruction in the condenser.

Acknowledgements

The present work is supported financially by the Ministry of Science, Research and Technology of Iran.

Nomenclature

Abbreviations

EVA	evaporator
HEX	heat exchanger
IHEX	internal heat exchanger
HTP	high temperature process
LTP	low temperature process
ORCC	ORC condenser
ORCP	ORC pump
ORCT	ORC turbine

Latin letters

e	specific physical exergy (J/kg)
$\dot{E}$	exergy flow rate (W)
h	specific enthalpy (J/kg)
$\dot{Q}$	heat transfer rate (W)
R	gas constant (J/kg K)
s	entropy (J/kg K)

T	temperature (K)
$\dot{W}$	power (W)

Greek letters

η	energy efficiency (-)
η_{is}	isentropic efficiency (-)
ε	exergy efficiency (-)

Subscripts

D	destruction
in	inlet conditions
is	isentropic
out	outlet conditions
ph	physical
0	ambient conditions

References

[1] T. V. Nguyen, L. Tock, P. Breuhaus, F. Maréchal, and B. Elmegaard, "Oil and gas platforms with steam bottoming cycles: System integration and thermoenvironomic evaluation," *Appl. Energy*, vol. 131, pp. 222–237, 2014.

[2] D. S. J. Jones, "Support systems common to most refineries," in *Handbook of Petroleum Processing*, Springer, Dordrecht, Netherlands, 2008, pp. 521–610.

[3] R. Vanner, "Energy use in offshore oil and gas production: trends and drivers for efficiency from 1975 to 2025," *Policy Stud. Inst. Work. Pap.*, September, 2005.

[4] L. Riboldi and L. O. Nord, "Concepts for lifetime efficient supply of power and heat to

offshore installations in the North Sea," *Energy Convers. Manag.*, vol. 148, pp. 860–875, 2017.

[5] M. J. Mazzetti, Y. Ladam, H. T. Walnum, B. L. Hagen, G. Skaugen, and P. Nekså, "Flexible combined heat and power systems for offshore oil and gas," *ASME 2014 Power Conf. (POWER2014-32169)*, pp. 1–8, 2014.

[6] M. Voldsund, I. S. Ertesvåg, W. He, and S. Kjelstrup, "Exergy analysis of the oil and gas processing on a north sea oil platform a real production day," *Energy*, vol. 55, pp. 716–727, 2013.

[7] T. V. Nguyen, L. Pierobon, B. Elmegaard, F. Haglind, P. Breuhaus, and M. Voldsund, "Exergetic assessment of energy systems on North Sea oil and gas platforms," *Energy*, vol. 62, pp. 23–36, 2013.

[8] S. de Oliveira Júnior and M. van Hombeeck, "Exergy analysis of petroleum separation processes in offshore platforms," *Energy Convers. Manag.*, vol. 38, no. 15–17, pp. 1577–1584, 1997.

[9] L. O. Nord and O. Bolland, "Steam bottoming cycles offshore - Challenges and possibilities," *J. Power Technol.*, vol. 92, no. 3, pp. 201--207, 2012.

[10] L. O. Nord and O. Bolland, "Design and off-design simulations of combined cycles for offshore oil and gas installations," *Appl. Therm. Eng.*, vol. 54, no. 1, pp. 85–91, 2013.

[11] H. T. Walnum, P. Nekså, L. O. Nord, and T. Andresen, "Modelling and simulation of CO_2 (carbon dioxide) bottoming cycles for offshore oil and gas installations at design and off-design conditions," *Energy*, vol. 59, pp. 513–520, 2013.

[12] L. Riboldi and L. O. Nord, “Lifetime Assessment of Combined Cycles for Cogeneration of Power and Heat in Offshore Oil and Gas Installations,” *Energies*, vol. 10, p. 744, 2017.

[13] B. F. Tchanche, G. Lambrinos, A. Frangoudakis, and G. Papadakis, “Low-grade heat conversion into power using organic Rankine cycles - A review of various applications,” *Renew. Sustain. Energy Rev.*, vol. 15, no. 8, pp. 3963–3979, 2011.

[14] S. Lecompte, H. Huisseune, M. van den Broek, B. Vanslambrouck, and M. de Paepe, “Review of organic Rankine cycle (ORC) architectures for waste heat recovery,” *Renew. Sustain. Energy Rev.*, vol. 47, pp. 448–461, 2015.

[15] F. Vélez, F. Chejne, G. Antolin, and A. Quijano, “Theoretical analysis of a transcritical power cycle for power generation from waste energy at low temperature heat source,” *Energy Convers. Manag.*, vol. 60, pp. 188–195, 2012.

[16] J. E. Barrera, E. Bazzo, and E. Kami, “Exergy analysis and energy improvement of a Brazilian floating oil platform using Organic Rankine Cycles,” *Energy*, vol. 88, pp. 67–79, 2015.

[17] L. Pierobon, T. V. Nguyen, U. Larsen, F. Haglind, and B. Elmegaard, “Multi-objective optimization of organic Rankine cycles for waste heat recovery: Application in an offshore platform,” *Energy*, vol. 58, pp. 538–549, 2013.

[18] V. Eveloy, P. Rodgers, and L. Qiu, “Performance investigation of a power, heating and seawater desalination poly-generation scheme in an off-shore oil field,” *Energy*, vol. 98, pp. 26–39, 2016.

[19] M. A. Khatita, T. S. Ahmed, F. H. Ashour, and I. M. Ismail, “Power generation using

waste heat recovery by organic Rankine cycle in oil and gas sector in Egypt: A case study," *Energy*, vol. 64, pp. 462–472, 2014.

[20] R. K. Bhargava, M. Bianchi, L. Branchini, A. De Pascale, and V. Orlandini, "Organic Rankine cycle system for effective energy recovery in offshore applications: a parametric investigation with different power rating gas turbines," *Proc. ASME Turbo Expo 2015 Turbine Tech. Conf. Expo. GT2015. June 15 – 19, 2015, Montréal, Canada*, pp. 1–13, 2015.

[21] J. A. M. da Silva and S. de Oliveira Júnior, "Unit exergy cost and CO_2 emissions of offshore petroleum production," *Energy*, vol. 147, pp. 757–766, 2018.

[22] Y. M. Barbosa, J. A. M. da Silva, S. de O. Junior, and E. A. Torres, "Performance assessment of primary petroleum production cogeneration plants," *Energy*, vol. 160, pp. 233–244, 2018.

[23] T. V. Nguyen, T. G. Fülöp, P. Breuhaus, and B. Elmegaard, "Life performance of oil and gas platforms: Site integration and thermodynamic evaluation," *Energy*, vol. 73, pp. 282–301, 2014.

[24] T. V. Nguyen, T. Jacyno, P. Breuhaus, M. Voldsund, and B. Elmegaard, "Thermodynamic analysis of an upstream petroleum plant operated on a mature field," *Energy*, vol. 68, pp. 454–469, 2014.

[25] A. B. Rian and I. S. Ertesvåg, "Exergy evaluation of the Arctic Snøhvit liquefied natural gas processing plant in northern Norway - Significance of ambient temperature," *Energy and Fuels*, vol. 26, no. 2, pp. 1259–1267, 2012.

[26] A. B. Rian and I. S. Ertesvåg, “Exergy analysis of a steam production and distribution system including alternatives to throttling and the single pressure steam production,” *Energy Convers. Manag.*, vol. 52, no. 1, pp. 703–712, 2011.

[27] Norwegian Meteorological Institute, "Daily normal values 1961-1990", eklima.met.no (visited 17 Sept 2018)

[28] L. Pierobon, R. Kandepu, and F. Haglind, “Waste Heat Recovery for Offshore Applications,” *Proc. ASME 2012 Int. Mech. Eng. Congr. Expo. MECE2012 Novemb. 9-15, 2012, Houston, Texas, USA*, pp. 1–10, 2012.

[29] A. Bejan and G. Tsatsaronis, *Thermal design and optimization*. John Wiley & Sons, 1996.

[30] P. Colonna, E. Casati, C. Trapp, T. Mathijssen, J. Larjola, T. Turunen-Saaresti, and A. Uusitalo, “Organic Rankine Cycle Power Systems: From the Concept to Current Technology, Applications, and an Outlook to the Future,” *J. Eng. Gas Turbines Power*, vol. 137, no. 10, p. 100801, 2015.

[31] E. Macchi and M. Astolfi, *Organic Rankine Cycle (ORC) Power Systems: Technologies and Applications*, 1st ed. Woodhead Publishing, 2016.

[32] F. Mohammadkhani, N. Shokati, S. M. S. Mahmoudi, M. Yari, and M. A. Rosen, “Exergoeconomic assessment and parametric study of a gas turbine-modular helium reactor combined with two organic Rankine cycles,” *Energy*, vol. 65, pp. 533–543, 2014.

[33] M. Yari, “Performance analysis of the different Organic Rankine Cycles (ORCs) using dry fluids,” *Int. J. Exergy*, vol. 6, no. 3, p. 323, 2009.

[34] M. Yari, “Exergetic analysis of various types of geothermal power plants,” *Renew.*

Energy, vol. 35, no. 1, pp. 112–121, 2010.

[35] H. D. Madhawa Hettiarachchi, M. Golubovic, W. M. Worek, and Y. Ikegami, "Optimum design criteria for an Organic Rankine cycle using low-temperature geothermal heat sources," *Energy*, vol. 32, no. 9, pp. 1698–1706, 2007.

[36] B.J. McBride, M. J. Zehe, S. Gordon, NASA Glenn coefficients for calculating thermodynamic properties of individual species, NASA/TP-2002-211556, Sept. 2002.

[37] Dow Chemical Company, "Material safety data sheet: DOWTHERM A Heat Transfer Fluid", http://www.dow.com/en-us (Last visited 9 Aug 2018).

[38] S. A. Klein and F. L. Alvarado, *EES: Engineering equation solver for the microsoft windows operating system*. F-Chart software, 1992.

[39] B. A. Younglove and M. O. McLinden, "An international standard equation of state for the thermodynamic properties of Refrigerant 123 (2,2-Dichloro-1,1,1-Trifluoroethane)," *J. Phys. Chem. Ref. Data*, vol. 23, no. 5, pp. 731–779, 1994

[40] F. J. Fernández, M. M. Prieto, and I. Suárez, "Thermodynamic analysis of high-temperature regenerative organic Rankine cycles using siloxanes as working fluids," *Energy*, vol. 36, no. 8, pp. 5239–5249, 2011.

[41] P. Colonna, N. R. Nannan, and A. Guardone, "Multiparameter equations of state for siloxanes: [(CH3)3-Si-O1/2]2-[O-Si-(CH3)2]i=1,...,3, and [O-Si-(CH3)2]6," *Fluid Phase Equilib.*, vol. 263, no. 2, pp. 115–130, 2008.

[42] P. Colonna, N. R. Nannan, A. Guardone, and E. W. Lemmon, "Multiparameter equations of state for selected siloxanes," *Fluid Phase Equilib.*, vol. 244, no. 2, pp. 193–211, 2006.

[43] Y. A. Çengel and M. A. Boles, Thermodynamics: An Engineering Approach, 4th ed, McGraw Hill, Boston, 2002.

[44] J. Szargut, D. R. Morris, and F. R. Steward, Exergy Analysis of Thermal, Chemical, and Metallurgical Processes, Hemisphere Pub, *Philadelphia., USA*, 1988.

[45] T. J. Kotas, The Exergy Method of Thermal Plant Analysis, 1st ed, Butterworths, London, 1998.

[46] M.J. Moran, H.N. Shapiro, D.D. Boettner and M.B. Bailey, Principles of Engineering Thermodynamics, 8th Ed., Wiley, 2015.

[47] H. Nami and E. Akrami, "Analysis of a gas turbine based hybrid system by utilizing energy, exergy and exergoeconomic methodologies for steam, power and hydrogen production," *Energy Convers. Manag.*, vol. 143, pp. 326–337, 2017.

[48] L.V. Gurvič, I.V. Vejc and C.B.Alcock, Thermodynamic Properties of Individual Substances Vol. 1 Part 2 Elements O,H(D,T),F, Cl, Br, I, He, Ne, Ar, Kr, Xe, Rn, S, N, P, and their compounds – Tables, 4th ed., Hemisphere Publ., New York, 1989.

[49] L.V. Gurvič, I.V. Vejc and C.B.Alcock, Thermodynamic Properties of Individual Substances Vol.2 Part 2 Elements C, Si, Ge, Sn, Pb, and their compounds – Tables, 4th ed., Hemisphere Publ., New York, 1991.

[50] Y.S. Touloukian and T. Makita, Thermophysical Properties of Matter Vol. 6 Specific Heat Nonmetallic Liquids and Gases, IFI/Plenum, New York, 1970.